JOURNAL OF OPTOELECTRONICS AND ADVANCED MATERIALS, Vol. 11, No. 4, April 2009, p. 473 - 478

Effect of silver nitrate ($AgNO_3$) on the optical, thermal and mechanical properties of γ-glycine single crystal

C. SEKAR*, R. PARIMALADEVI
Department of Physics, Periyar University, Salem – 636 011, Tamilnadu, India

Single crystal of $AgNO_3$ doped γ-glycine, a nonlinear optical (NLO) material have been grown by slow evaporation method. The phase purity and crystal structure of the grown crystals have been confirmed by powder X-ray diffraction studies. Thermal analysis was carried out to study the effect of $AgNO_3$ doping on thermal stability of γ-glycine crystal. Functional groups of the grown crystal were identified through FTIR and FT-Raman spectroscopy. The optical transparency and lower cut off value of UV transmission were ascertained by recorded UV- Visible spectrum of γ-glycine crystals. The existence of second harmonic generation (SHG) of the grown crystal was confirmed by Kurtz-powder technique and the efficiency of frequency doubling was found to be 1.4 times than that of KDP. Mechanical property of the grown $AgNO_3$ doped γ-glycine crystal was studied by Vickers microhardness tester.

(Received March 14, 2009; accepted April 23, 2009)

Keywords: Nonlinear optical materials, γ-glycine, Growth from solution, Vibrational spectroscopy, Thermal properties

1. Introduction

The search for non-linear optical (NLO) material has been of great interest in recent years due to their widespread applications such as high-speed information processing, optical communications and optical data storage [1]. Within the last decade much progress has been made in the development of these NLO organic materials having large nonlinear optical coefficients. One of the advantages in working with organic materials is that they allow one to fine-tune the chemical structures and properties for the desired nonlinear optical properties. In addition, the organic crystals have large optical susceptibility, inherent ultra fast response times and high optical threshold for laser power as compared with inorganic materials. Moreover, their lower cut off wavelengths and a wide transparency window in the visible region makes the candidate materials subject for extensive investigation [2]. Aminoacids are interesting materials for NLO application as they contain proton donar carboxyl acid (-COO) group and the proton acceptor amino (NH_2) group in them [3]. Especially some aminoacids like arginine, lysine, l-alanine and γ-glycine are evidently showing NLO activity because they have a donar NH_2 group and acceptor COOH group and also intermediate charge transfer was possible.

Glycine, the simplest aminoacid, has three polymeric crystalline forms: α, β and γ. Both α and β forms crystallize in centrosymmetric space group $P2_1/c$. γ-glycine crystallizes in non-centrosymmetric space group $P3_1$ making it a candidate for piezo-electric and NLO applications [4, 5]. The metastable α-glycine grown from aqueous solution transforms into γ-form spontaneously. The least stable β-form is always obtained from water-alcohol mixed solvent. The β- form transforms rapidly to α- and γ- forms in presence of moisture at room temperature. The more stable γ-glycine crystals are grown from aqueous solution or gel in the presence of additives. The γ-form transforms to α form on heating around 170ºC [6]. Narayan Bhat et.al [6] reported that the morphology of the glycine crystals grown from various solvents such as sodium hydroxide, sodium fluoride, sodium nitrate and sodium acetate showed a marked difference in transition temperature and second harmonic conversion (SHG) efficiency. The SHG efficiency of γ-glycine grown in presence of NaF, NaOH and $NaCH_2COOH$ were reported to be 1.3, 1.4 and 1.2 times higher than that of potassium dihydrogen phosphate (KDP) crystal. The same authors have reported that the γ-crystal grown from a mixture of glycine and NaOH undergoes a transition from γ to α form at 172°C. Choudary et.al [7] has studied the low temperature ferroelectric phase transition of glycine silver nitrate (GSN) single crystals. Since silver nitrate crystal can crystallize in non-centrosymmetric space group and it has high transmission range, in present work, we choose silver nitrate as dopant and studied the optical property of $AgNO_3$ doped γ-glycine crystals for the first time.

2. Experimental

The α-glycine was crystallized by taking the analar grade 1M glycine (99%). In another series γ-glycine was synthesized by taking 1M glycine with two different concentration of silver nitrate (0.1 and 0.2M). Impurity content in glycine and γ-glycine was minimized by successive recrystallization process. The pH value of the saturated glycine solution was found to be 4. In case of $AgNO_3$ added glycine solution, the pH values increased with increase in silver nitrate concentrations; 4.80 and 5.34 for 0.1 and 0.2 M respectively. As the growth rate of a crystal depends on solubility and growth temperature, the solubility of glycine and γ-glycine synthesized in presence of various concentration of $AgNO_3$ in double distilled water were determined at various temperatures [Fig.1]. It can be seen that the solubility of α-glycine was higher than that of γ-glycine. Moreover, the solubility increases with increase in temperature and decreases with increase in concentration of $AgNO_3$. This result confirms that the γ-glycine grown in presence of $AgNO_3$ was stable and less water soluble than glycine at room temperature. In both cases, positive slope of the solubility curve enables growth by slow evaporation method. The final solution was filtered using 0.1 micron porosity filter papers and kept in beakers covered with perforated sheets. The spontaneous evaporation of the solvent at room temperature yielded crystals in the time span of 15-20 days. The grown crystals were carefully harvested and then subjected to characterization studies.

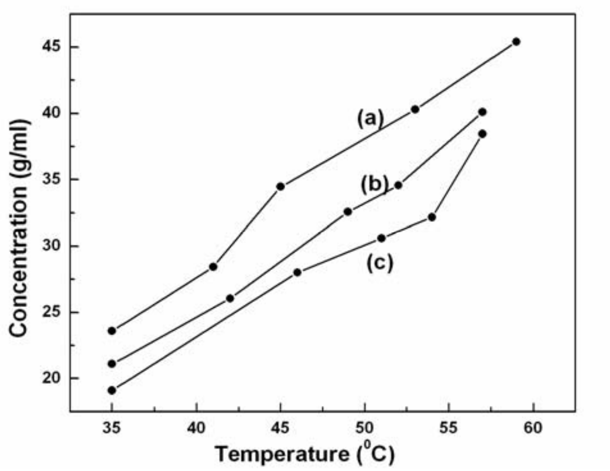

Fig. 1. Solubility curves of glycine (a) without and with incorporation of $AgNO_3$ (b) 0.1M (c) 0.2M.

Glycine crystals grown with silver nitrate were powdered and mixed with KBr pellets for obtaining transmission spectra in the mid IR region (4000-400cm^{-1}) using Perkin Elmer (Spectrum RX1) and FT Raman spectra was recorded using NEXUS670. Powder XRD pattern was recorded on Bruker diffractometer within the 2θ range of 10 to 80° using CuKα as X-ray source (λ = 1.5406Å) to confirm crystal quality and to identify the cell parameters. Thermogravimetry of samples was performed using TA instruments SDT Q600 V8.3. UV - Visible spectrum was recorded on a PerkinElmer Lambda 25 spectrometer in transmission mode. Second harmonic generation efficiency of the samples was determined using Kurtz powder method. A Q switched Nd:YAG laser beam of wavelength 1064nm was used with an input energy of 1.35MJ/pulse and pulse width of 8ns, the repetition rate being 10Hz. The SHG radiations of 532 nm (green light) emitted were collected by a photo multiplier tube (PMT-Philips photonics model 8563) and the optical signal incident on the PMT was converted into voltage output at the CRO (Tektronix –TDS 3052B). Microhardness measurements were carried out on the grown crystals using Shimadzu tester.

3. Results and discussion

3.1 Crystal growth

Figs. 2 & 3 show the crystal habits of γ- glycine grown in presence of $AgNO_3$ (0.1M and 0.2M) respectively. The crystals grown in presence of lower concentration of $AgNO_3$ (0.1M) shows prismatic shape as like α-glycine reported by Dawson et.al [8]. Morphology of the 0.2M $AgNO_3$ doped crystals changed significantly when compared to that of pure glycine. When the crystal face has a structure similar to that of a face of the crystal of the adsorbed substance a particle of the latter will adhere to the crystal face just as it would happen with the corresponding face of its own crystal, since it experiences similar forces. Thus, on the growing face, impurity particles are strongly adsorbed together with particles of the main substances [9]. Upon further increase in concentration, silver nitrate affects the growth rate of the crystal faces through incorporation into the lattice, disturbing crystal arrangement. Thus the crystal morphology of glycine crystal grown in the presence of 0.2M of $AgNO_3$ changed to bipyramids. Also, there is a significant change in the color of the crystal due to the silver nitrate doping i.e., γ-glycine grown in presence of $AgNO_3$ was brown in color. In both the cases, the crystals were transparent.

Fig. 2. As grown 0.1 M $AgNO_3$ doped γ-glycine crystal.

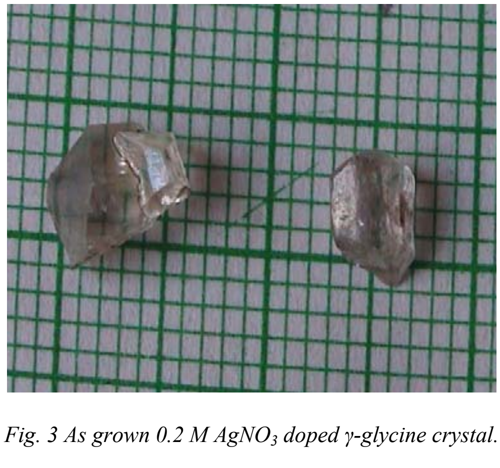

Fig. 3 As grown 0.2 M $AgNO_3$ doped γ-glycine crystal.

3.2. X-Ray Diffraction Analysis

The crystal structure of glycine was reported by Dawson et.al [8]. The γ-glycine crystallizes in hexagonal structure with space groups of $P3_1$. X-ray powder diffraction patterns of the grown crystals were shown in Fig. 4. The results agree well with the simulated XRD pattern of pure γ-glycine and the characteristic peaks have appeared at around 25.3° (2θ). Slight shift in the peak position may be due to doping of $AgNO_3$ in γ-glycine crystal. Appearance of sharp and strong peaks confirms the good crystallinity of the grown samples. The estimated lattice parameters of γ-glycine grown with incorporation of various concentration of $AgNO_3$ were given in Table 1.

Table1. Lattice parameters of γ-glycine grown with various concentration of $AgNO_3$.

$AgNO_3$ concentration selected for growing γ-glycine	Lattice parameters a = b (Å)	c (Å)
0.0M[a]	6.86	5.43
0.1M[b]	6.88	5.40
0.2M[b]	7.04	5.36

a , Dawson et.al [8]; b, present work

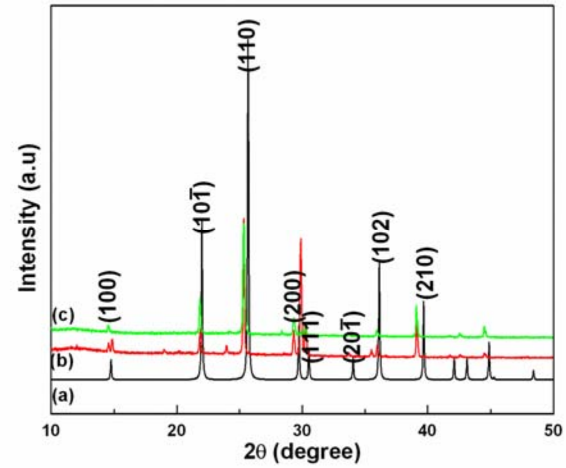

Fig.4. (a) Calculated XRD pattern of γ-glycine and experimental powder XRD pattern of γ-glycine grown in presence of (b) 0.1M (c) 0.2M of $AgNO_3$.

3.3 Thermal analysis

Figs.5 and 6 illustrate the TG-DTA curves of 0.1M and 0.2M $AgNO_3$ doped γ-glycine crystals respectively. The experiments were performed in the temperature range of 30°-1100°C in nitrogen atmosphere and the heating rate was 20°C/min. The TGA curves show no change in weight before 215°C for all samples, which eliminate the possibility of hydrate or solvate incorporation into crystals. The major weight loss (~35%) occurred in the temperature range between 230-300°C which could be attributed to the sublimation and decomposition of the samples resulting in the release of NH_3 and CO molecules. Appearance of a peak at temperature 170°C in DTA curve of 0.1M $AgNO_3$ doped γ-glycine crystal corresponds to the phase transformation of γ- to α-phase. This transition temperature got increased to 208°C for the doped crystal (0.2 M $AgNO_3$). This improvement in transition temperature could be attributed to the $AgNO_3$ doping into γ-glycine. Moreover, there is a significant difference in the weight loss pattern between 0.1 M doped and 0.2M doped γ- glycine at higher temperatures. These results confirmed that the silver nitrate is doped into γ-glycine crystal though the precise dopant concentrations were not measured directly. The DTA curve of $AgNO_3$ doped γ-glycine reveals no endothermic/exothermic peak below 207°C suggesting its structure stability in the temperature range. This ensures the suitability of the material for possible application in laser, where the crystal is required to withstand high temperature.

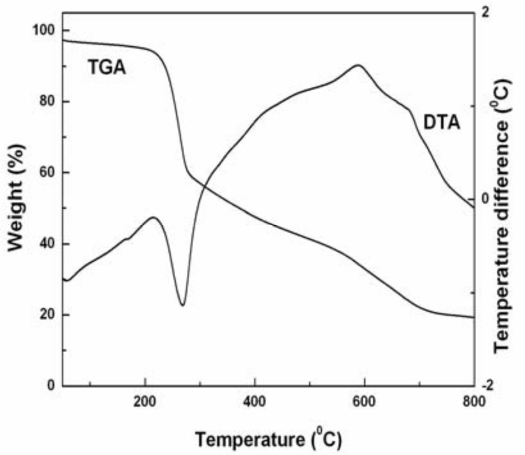

Fig.5. TG-DTA curve $AgNO_3$ (0.1M) doped γ-glycine crystal.

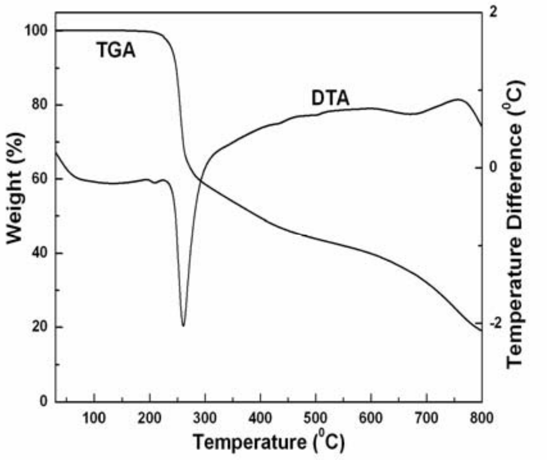

Fig.6. TG-DTA curve of $AgNO_3$ (0.2M) doped γ-glycine crystal.

3.4 FTIR and FT-Raman Analyses

The FTIR and FT- Raman spectra of powdered glycine grown with $AgNO_3$ were shown in the Figs. 7 & 8 respectively. Though $AgNO_3$ concentration in the grown crystals was not quantitatively measured it was indirectly studied by these spectral analyses. The observed wave numbers, relative intensities obtained from the recorded spectra and the assignments proposed for both crystals were found to be in good agreement with the assignment proposed in reported literature [10, 11] and are listed in Table 2. In FTIR spectra broad envelope in the higher wavenumber region between 3700- 2100 cm^{-1} was due to hydrogen interaction with other atoms such as N-H stretching of NH_2 and C-H of CH_2 stretching. The broad nature of this region became narrow in 0.2M $AgNO_3$ doped crystals. The peak observed at 2989cm^{-1} in Raman spectra was due to C-H stretching. Two overlapped bands at around 1612 cm^{-1} and 1404 cm^{-1} in FTIR spectra were attributed to the asymmetric and symmetric stretch mode of the COO^- group. While increasing dopant (0.2M) concentration this peak was shifted to 1634 cm^{-1} and 1399 cm^{-1} respectively. Other bands of COO^- deformation mode were observed at 690 and 502 cm^{-1}.

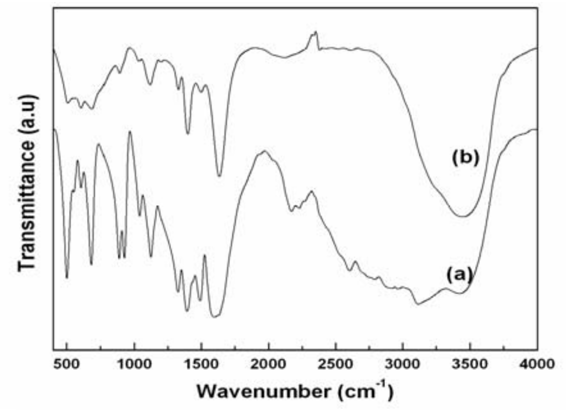

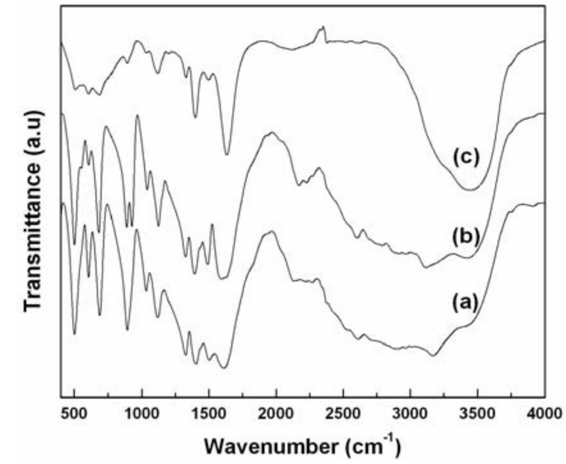

Fig.7. FTIR spectra of (a) α- glycine and γ - glycine crystal grown in presence of (b) 0.1M (c) 0.2M of $AgNO_3$

These bands were seen at 687 and 506 cm^{-1} in the Raman spectra. Both the results confirmed that the glycine molecule existed in zwitterions form inside the crystal. This caused an antiparallel arrangement, which contributed to non-centrosymmetric crystalline growth. Choudary et.al [7] reported that silver ion bridge the centrosymmetrically related carboxyl groups (COO^-) to form dimers. The medium intensity peak at 1033 cm^{-1} related to C-C-N asymmetric stretching became weak and got shifted to 1049 cm^{-1} in the doped GG crystal. The characteristics peak of GG crystal observed at 927 cm^{-1} for 0.1M $AgNO_3$ doped crystal got shifted to 905 cm^{-1} for 0.2M doped GG crystal. In Raman spectra vibration due to CCN stretching observed at 387 and 319 cm^{-1} for 0.1M doped crystal got shifted to 341 and 309 cm^{-1} for 0.2M doped crystal which confirmed the $AgNO_3$ doping into the target compound.

In Raman spectra there was a significant increase in peak intensities of the 0.2M $AgNO_3$ doped crystal when compared to that of 0.1M doped crystal. In addition major shifts with known frequency and additional peaks corresponding to the internal modes in the mid region have been observed in this study. This proves that the $AgNO_3$ was doped into γ-glycine crystal and the dopant concentration increases with the increase in starting compound.

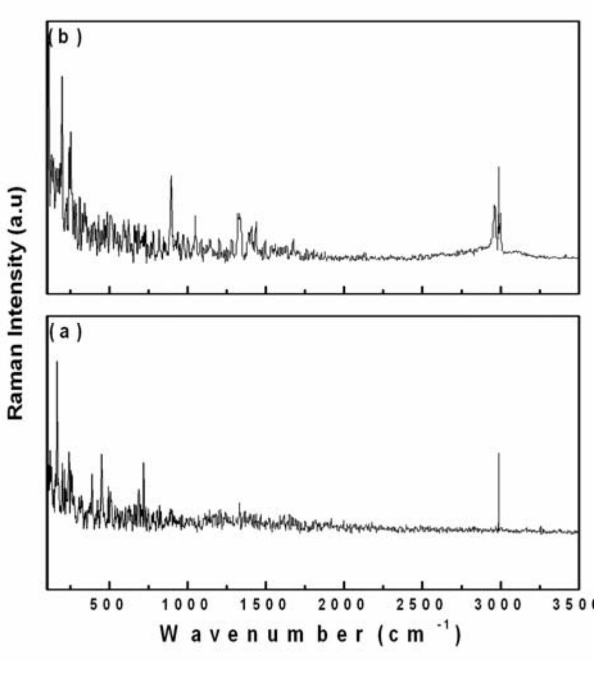

Fig.8. FT-Raman spectra of γ-glycine crystal grown in presence of (a) 0.1M (b) 0.2M of $AgNO_3$.

Table 2 Observed IR and Raman wavenumbers (cm^{-1}) of α-glycine and γ - glycine grown in presence $AgNO_3$.

α- glycine FTIR	γ - glycine grown in presence of 0.1M $AgNO_3$ FTIR FT-Raman	γ - glycine grown in presence of 0.2M $AgNO_3$ FTIR FT-Raman	Tentative assignment
3908w	3422s	3433s	$\nu_{as}(NH_3)^+$
	3119s		
3171s	2989m	2989m	$\nu_s(NH_3)^+$
2899m		2963w	
	2792m		ν_{as} (C-H)
	2604m	2617w	
2612m	2228w	2381w	ν_s (C-H)
2270m	2172w	2121w	
2135w	1597vs	1634m	
1612vs	1492s	1498w	
1502s		1438w	ν (N-H-O)
	1394s	1399m	
1404s	1327s	1330w	
1328s	1331w	1322w	
1119m	1125m	1119w	$\nu_{as}(COO^-)$
1033m	1041w	-	
		905w	δ (NH_3)
	927 m		
892m		892w	δ (CH_2)
690m		687w	$\nu_s(COO^-)$
607w	888 m	686w	
		607w	ω (CH_2)
	718m	621w	
			ρ (NH_3)
502m	684m	592w	
	687w		ν_{as} (CCN)
		509w	
	607w	506w	characteristic peak of GG
		485w	
	502m	450w	ν_s (CCN)
	506w		
		428w	-
	492w		
		341w	δ (COO^-)
	450m		
		309w	ω (COO^-)
	423w		
		285-127	
	387m		
		109vs	ρ (COO^-)
	319w		
			ρ (COO^-)
	252-119		
	101m		
			δ (CCN)
			δ (CCN)
			Lattice modes
			τ (C-C)

ν, stretching; ρ, rocking; δ,deformation; ω, wagging, τ, torsion;w, weak; m, medium, s, strong, vs, very strong.

3.5 Optical transmission spectral analysis

Good optical transmittance and lower cut off wavelengths are very important properties for NLO crystals. In these crystals the UV- Visible range from 200 to 400 nm is very important for the realization of SHG output in this range using diode and solid-state lasers. The UV transmission spectrum of γ- glycine and $AgNO_3$ doped γ-glycine is shown in Figs.9 & 10. It can be seen from the transmission curve that the lower cutoff wavelength lies nearly 320 and 230 nm for γ-glycine and $AgNO_3$ doped γ-glycine crystals make potential material for frequency doubling. Thus lower cut off value changed from near UV region (320nm) to middle UV region (230nm) and this may be due to $AgNO_3$ doping. The absence of absorption in the visible region clearly indicates that the grown crystal can be used for optoelectronic applications. High transmittance % is observed from 500 nm which, clearly indicates the crystal possess good optical transparency for SHG of Nd:YAG laser.

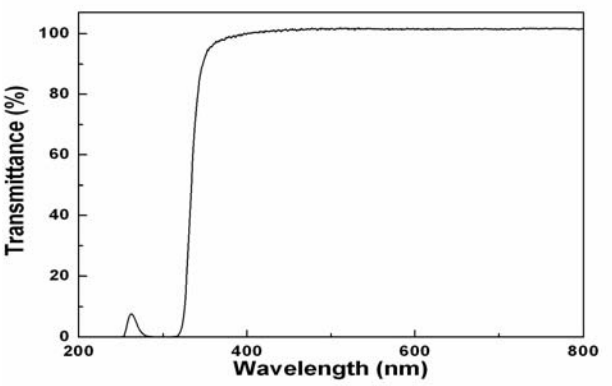

Fig.9. UV- Visible spectra of γ-glycine

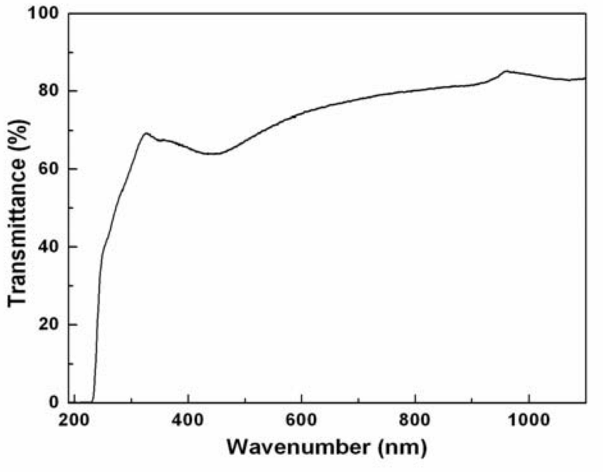

Fig.10. UV- Visible spectra of $AgNO_3$ doped γ-glycine

3.6 Powder SHG measurement

In order to confirm the NLO property, the grown crystals were powdered and subjected to Kurtz and Perry powder technique, which remains powerful tool for initial screening of materials for SHG [12]. The second harmonic signal generated in the crystalline sample was confirmed from the emission of green radiation (λ = 534nm) from the crystal. The measured amplitude of second harmonic green light for $AgNO_3$ doped γ-glycine is 135mV against 95mV for KDP crystal. The result obtained shows a powder SHG efficiency of $AgNO_3$ doped γ-glycine is about 1.4 times that of potassium dihydrogen orthophosphate. This may be due to central ion in metal organic complex offers a certain anisotropic field to keep NLO active chromopores which drastically vary the hyperpolarizibility value [13].

3.7 Vickers Microhardness Studies

Hardness is a measure of materials' resistance to localized plastic deformation. It plays key role in device fabrication. The mechanical property of γ-glycine and $AgNO_3$ doped γ-glycine crystals was studied by Vickers hardness test. The applied loads were 25, 50,100 and 200 grams.

The micro hardness was calculated using the relation $Hv = 1.8544\ P/d^2$ (kg/mm^2) where P is the applied load and d is the diagonal length of the indentation impression.

The calculated Vickers hardness values for pure and $AgNO_3$ doped γ-glycine crystals as a function of load was shown in Fig. 11 Vickers Hardness values of doped crystals are higher than that of pure sample. It can be noticed that the doped crystal has higher Hv value (38 kg/mm^2) than that of pure crystal (10 kg/mm^2). The hardness values of both pure and doped crystals increase with increasing load. The reverse indentation size effect involves increase in hardness value with increasing load [14]. In the doped crystal a crack developed on the surface upon applying the load of 200 g where as the undoped crystal broke at 100 g itself. This result confirmed that the $AgNO_3$ doping into γ-glycine improves its hardness.

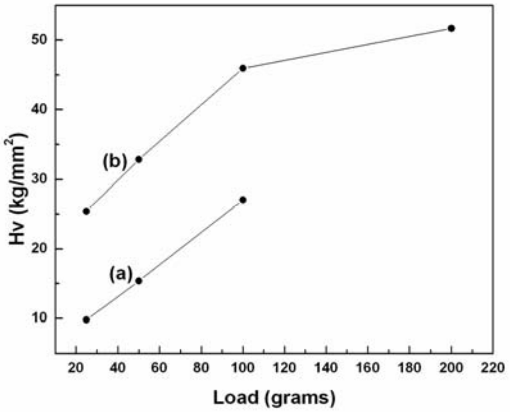

Fig.11 Vickers Hardness of (a) γ-glycine (b) $AgNO_3$ doped γ-glycine

4. Conclusion

Optically transparent single crystal of $AgNO_3$ doped γ-glycine was conveniently grown by slow-evaporation method. The crystals were transparent and their shape and size were sensitive to the amount of dopant present in the solution during growth. Silver nitrate as a dopant has been found to yield crystals useful for NLO application. Powder XRD, TG-DTA, FTIR and FT-Raman studies confirmed that the $AgNO_3$ was doped into γ-glycine. Kurtz powder SHG test confirmed the frequency doubling of the grown crystal and its efficiency was 1.4 times higher than that of KDP. Owing to its wide transparency range, high thermal stability, high hardness value with relatively high SHG efficiency make $AgNO_3$ doped γ-glycine a promising material for laser application and fabrication of electro-optic devices.

Acknowledgements

One of the authors (R.P) thanks Periyar University for providing University Research Fellowship (URF) and the authors thank Prof. V. Krishnakumar of Periyar University and Dr. A. Thamizhavel of Tata Institute of Fundamental Research for their help in characterization.

References

[1] Yun Zhang, Hua Li, Bin Li, Yunxia Che, Jimin Zheng, Mater. Chem. Phys. **108,** 192 (2008).
[2] Shankang Gao, Weijun Chen, Guimel Wang, Jianzhong Chen, J. Cryst. Growth **297,** 361 (2006).
[3] Tapati Mallik, Tanusree Kar, J Cryst. Growth **285,** 178 (2005).
[4] Xia Yang, Jie Lu, Xiu-Juan Wang, Chi- Bun Ching, J. Cryst. Growth **310**, 604 (2008).
[5] K. Ambujam, S. Selvakumar, D. Prem Anand, G. Mohamed, P. Sagayaraj, Cryst Res. Technol. **41**, 671 (2006).
[6] M. Narayanan Bhat, S. M. Dharmaprakash, J. Cryst. Growth **242**, 245 (2002).
[7] Rajul Rajan Choudary, Lata Panicker, R. Chitra, T. Sakuntala, Solid State Commun.**145,**407 (2008).
[8] Alice Dawson, David R. Allan, Scott A. Belmonte, Stewart J. Clark, William I. F. David, Pamela A. McGregor, Simon Parsons, Colin R. Pulham, Lindsay Sawyer, Cryst Growth Des. **5,** 1415 (2005).
[9] A.S. Haja Hammed, G. Ravi, R. Jayavel, P. Ramasamy, J Cryst. Growth **250,** 126 (2003).
[10] Mario T. Rasoda, Maria Leonor, T.S. Duarte, Rui Fausto, Vibration. Spectrosc.**16,** 35 (1998).
[11] Hans Stenback, J. Raman Spectrosc. **5**, 49 (1976).
[12] S. K. Kurtz, T.T. Perry, J. Appl. Phys. **39,** 3798 (1968).
[13] V. Krisnakumar, R. Nagalakshmi, Spectrochim. Acta Part A **68,** 443 (2007).
[14] T. Kangasekaran, P. Mythili, P. Srinivasan, N. Vijayan, G. Bhagavannarayana, P.K. Kulriya, D. Kanjilal, R. Gopalakrishnan, P. Ramasamy, Cry. Res.Tech. **42,** 1376 (2007).

---

*Corresponding author: sekar2025@gmail.com